ORAL/POSTER REFERENCE: ICF100409PR

FRACTURE INITIATION AND CRACK GROWTH – COHESIVE ZONE MODELING AND STEREOSCOPIC MEASUREMENTS

C.R. Chen[1*], I. Scheider[2], T. Siegmund[3], A. Tatschl[4], O. Kolednik[4] and F.D. Fischer[1]

[1] Institute of Mechanics, Montanuniversität, A - 8700 Leoben, Austria
[2] GKSS Forschungszentrum Geesthacht GmbH, D - 21502 Geesthacht, Germany
[3] School of Mechanical Engineering, Purdue University, West Lafayette, IN 47907-1288, USA
[4] Erich Schmid Institute of Materials Science, Austrian Academy of Sciences, A - 8700 Leoben, Austria

ABSTRACT

The purpose of this paper is to study the application of a cohesive zone model, which is appropriate for the use with 3D-elements, for the numerical simulation of the crack growth in a Compact Tension specimen made of a mild steel. The main problem is how the two parameters which control the crack growth in the model, the cohesive energy Γ_0 and the cohesive strength T_{max}, can be determined. A procedure is proposed to determine the variation of the parameters along the crack front, $\Gamma_0(z)$ and $T_{max}(z)$, by using the local crack growth data in the specimen center and at the side surfaces and 2D modeling under plane strain and plane stress conditions, as well as the measurement of the variation of the critical crack tip opening displacement, $COD_i(z)$, along the crack front. The comparison between the experimental data and the numerical simulation reveals that the parameters of the cohesive zone model change during (the first stages of) crack extension.

KEYWORDS

numerical simulation, 3D cohesive zone model, cohesive strength, fracture initiation, crack growth, critical crack tip opening displacement, automatic fracture surface analysis, stereophotogrammetry

INTRODUCTION

The cohesive zone model has been increasingly applied for the numerical analysis of crack propagation, first, only for brittle materials that exhibit cleavage fracture and, later, also for tough materials which fail in a micro-ductile mode [1]. It uses a traction-separation law, i.e. a special curve relating the separation stress, T, to the displacement, δ, to model the behavior of the material in the process zone in front of the crack tip. The various traction-separation laws for micro-ductile crack growth have a common feature: with the increase of separation the traction increases, reaches the peak value, called the cohesive strength, T_{max}, and then decreases to zero when the separation reaches a critical value, δ_0. The area under the traction-separation curve is the separation energy, Γ_0, which represents physically the specific work required for the formation of the dimple structures on the two fracture surfaces [2]. It has been found that the exact shape of the T-δ curve has little effect on the crack growth behavior [3]; important are the magnitudes of the parameters T_{max} and Γ_0.
In the application of the cohesive zone model to ductile fracture, most studies have been performed under either plane strain or plane stress conditions. However, to model the crack growth in a specimen with smooth

[*] on leave from the Institute of Metal Research,Chinese Academy of Sciences, Shenyang, China

side-surfaces, a tri-dimensional (3D) cohesive zone model is necessary. Although it is conceptually not more complicated, the 3D case is more difficult from the numerical point of view. Some applications of a 3D cohesive zone model can already be found in literature, e.g., [4,5]. However, there still remains the problem how to select the variation of the parameters T_{max} and Γ_0 in the 3D case, since it has been shown in numerical investigations that T_{max} and Γ_0 are no material constants. It has been tried to relate them to either the local equivalent plastic strain [6], the local void volume fraction [7], or the local stress triaxiality, e.g., [8,9,10]. The latter idea seems to be especially promising; however, it is not known whether the stress triaxiality is the only factor influencing T_{max} and Γ_0. The current paper is devoted to this problem.

A 3D COHESIVE ZONE MODEL AND A FRACTURE MECHANICS EXPERIMENT

The experimental data of a multi-specimen J_{IC}-test, [11], shall be used to calibrate the parameters T_{max} and Γ_0 for a 3D cohesive zone model. The specimens were CT-specimens (thickness $B=25$ mm, width $W=50$ mm, initial crack length $a_0=27$ mm), the material was an annealed mild steel (yield strength $\sigma_y=270$ MPa, ultimate tensile strength $\sigma_u=426$ MPa) with a distribution of MnS inclusions which determine the micro-ductile fracture process. It is important to note that no shear lips are seen on the fracture surfaces. The crack extension, Δa, was measured on 9 equidistant positions; near the side surface, additional measurements were made. In total, 14 specimens were analyzed. The experiment was performed to study the near-initiation stage of crack growth; many data were taken at small crack growth values. The test gave a valid $J_{IC} = 120$ kJ/m^2; the physical crack extension in the center region begins much earlier, $J_i = 39$ kJ/m^2 [10].
From these data, curves of the local crack extension can be plotted against the load line displacement, $\Delta a(z)$-v_{LL} curves; z gives the position along the crack front, i.e., the distance from the midsection. Such curves were already used in the past to control the crack extension in conventional 3D-numerical studies where the variation of the crack tip opening displacement[1], CTOD, during crack extension was investigated, e.g. [12].
For the current numerical modeling, a 3D cohesive zone model has been implemented, [13], into the finite element (FE) system ABAQUS [14]. The details can be found elsewhere [15]. It is possible to use different traction-separation laws that consider both normal and shear components of fracture. For the current simulation, a cubic traction-separation law, [1], is applied. As we observe only Mode I fracture in the test, only the normal components of separation are relevant:

$$T(\delta) = \frac{27}{4} T_{\max} \left(\frac{\delta}{\delta_0} \right) \left[1 - 2 \left(\frac{\delta}{\delta_0} \right) + \left(\frac{\delta}{\delta_0} \right)^2 \right] \quad . \tag{1}$$

The integration of the curve yields the separation energy,

$$\Gamma_0 = \frac{9}{16} T_{\max} \delta_0 \quad . \tag{2}$$

The FE model consist of 9 layers of 8-node 3D solid elements through the half-thickness of the specimen. The width of the layers decreases near the side surface. The cohesive elements are placed at the crack plane. The element size in the direction of crack extension near the crack tip is 0.05 mm, further away 0.1 and 0.2 mm, respectively. The loading is performed by prescribing the load line displacement, v_{LL}.

THE CALIBRATION OF THE COHESIVE ZONE PARAMETERS FOR 2D MODELING

For 2D computations under plane strain conditions, the data of the local crack extension in the midsection, $\Delta a(z=0)$, can be used to select the appropriate cohesive element parameters $T_{max}^{(pl\varepsilon)}$ and $\Gamma_0^{(pl\varepsilon)}$, see Figure 1a. Figure 2a demonstrates that an increase of T_{max} (at fixed Γ_0) leads to a flatter Δa-v_{LL} curve; however, it does not influence the load line displacement at the point of fracture initiation, $v_{LL}^{(i)}$. An increase of Γ_0 (at fixed T_{max}) results in both a higher value of v_{LL} at initiation, $v_{LL}^{(i)}$ and a flatter Δa-v_{LL} curve, Figure 2b. This

[1] The crack tip opening displacement measured at the actual tip of (a growing) crack is designated *CTOD*; the value measured at the position of the initial crack front after the pre-fatigue is designated *COD*.

enables us to find the values $T_{max}^{(pl\sigma)} = 1100$ MPa and $\Gamma_0^{(pl\sigma)} = 11.5$ kJ/m^2 which give the best fit to the data. The accuracy of these values is good, say about 5%.

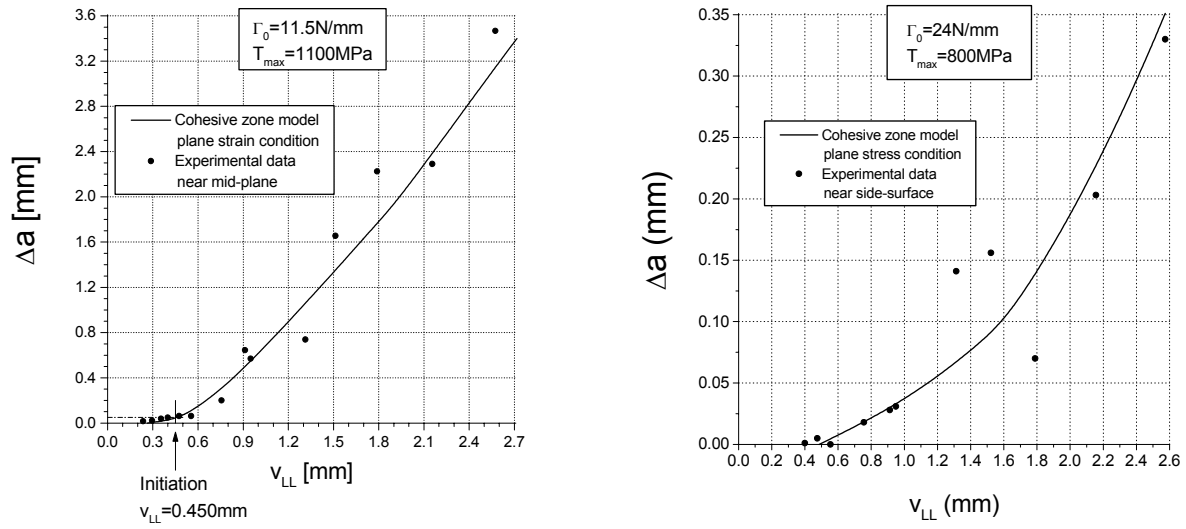

Figure 1: Local crack extension, Δa, versus load line displacement, v_{LL}. (a) Experimental data from the midsection and plane strain computation, (b) data from the side surface and plane stress computation.

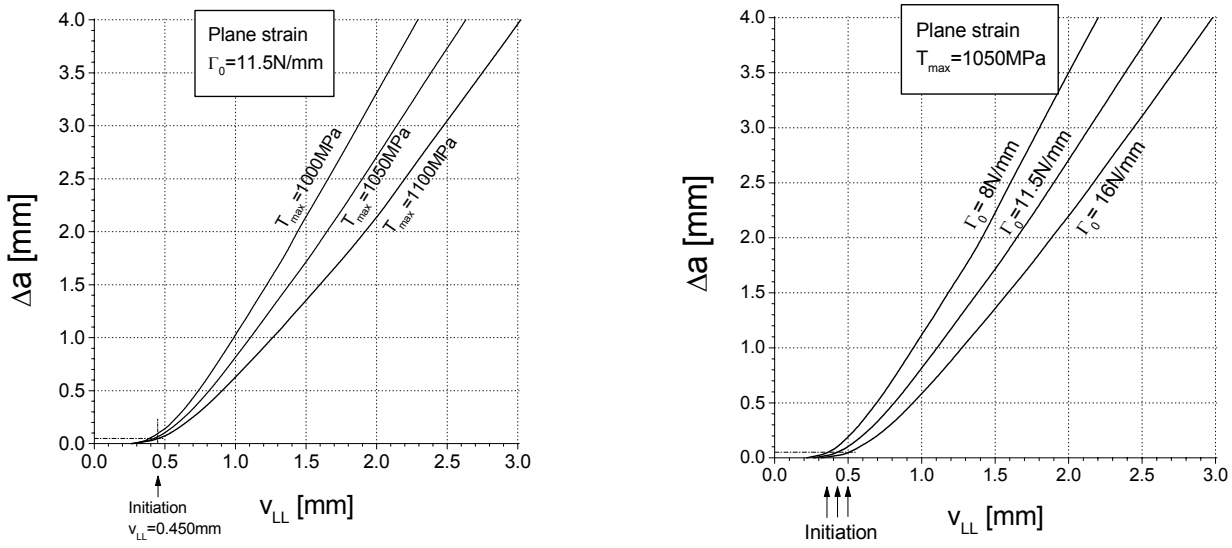

Figure 2: Influence of (a) the cohesive strength, T_{max}, and (b) the cohesive energy, Γ_0, on the Δa-v_{LL} curve for plane strain conditions.

Similarly, a 2D computation under plane stress conditions and the data of the local crack extension near the side surface, $\Delta a(z=12.5)$, can be used to find $T_{max}^{(pl\sigma)} \approx 800$ MPa and $\Gamma_0^{(pl\sigma)} = 24$ kJ/m^2 (Figure 1b). Because of the large scatter of the data, the accuracy is worse than for the plane strain case. T_{max} might be especially inaccurate, as in the plane stress case the separation strength does not have a large effect on the Δa-v_{LL} curve. Figure 3 shows the resulting J-integral versus crack extension (J-Δa) curves. These curves and the J-values at fracture initiation, $J_i^{(pl\varepsilon)} = 40$ kJ/m^2 and $J_i^{(pl\sigma)} = 85$ kJ/m^2, are similar to those obtained by a sandwich layer model [16]. From Eqn. 2, the values of the critical separation can be calculated, $\delta_0^{(pl\varepsilon)} = 0.020$ mm and $\delta_0^{(pl\sigma)} = 0.056$ mm. The J_i-values are much higher than the separation energies. This has been expected because at fracture initiation the plastic zone exceeds the process zone already by 2 orders of magnitude, $r_{y,i}^{(pl\varepsilon)} = 4.8$ mm. It is interesting to note that the ratio $J_i^{(pl\sigma)}/J_i^{(pl\varepsilon)} \approx 2.1$ comes close to the ratio of the separation energies $\Gamma_0^{(pl\sigma)}/\Gamma_0^{(pl\varepsilon)} \approx 2.2$. For the same material, in [17] the energy dissipation rate, i.e., the total non-reversible energy for a unit-area crack growth, was estimated for plane strain conditions assuming the

criterion *CTOA = constan*t and plane strain conditions. It was found that $D \approx constant \approx 1160$ kJ/m^2, i.e., by a factor 100 larger than the separation energy.

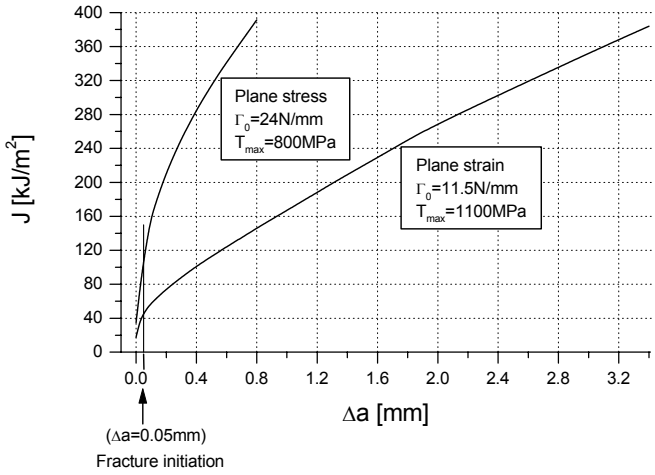

Figure 3: *J*-integral, *J*, versus mean crack extension, Δa, curves computed by the 2D cohesive zone models.

For 2D cohesive zone modeling, the calibration of the parameters poses no serious problem. No hint has been found that for our material the parameters change with the crack extension. However, the maximum Δa values are small, *4* mm in the midsection and *0.34* mm at the side surface.

ON THE CALIBRATION OF THE COHESIVE ZONE PARAMETERS FOR 3D MODELING

In the 3D case, the cohesive parameters are expected to vary along the crack front. An additional variation during crack extension is assumed to be small (see above). The calibration is much more difficult because a change of the parameters in one layer will affect the crack growth in all the other layers.
The first trial is to use cohesive parameters that are constant throughout the whole specimen. In Figure 4a an example is presented for $\Gamma_0 = 17.5$ kJ/m^2 and $T_{max} = 1100$ MPa. In the figure, the experimentally measured $\Delta a(z)$-values for three different load line displacements, v_{LL}, are compared to the computed Δa-distribution. The local crack extension decreases near the side surface but the result is not especially satisfying, see the discussion below.

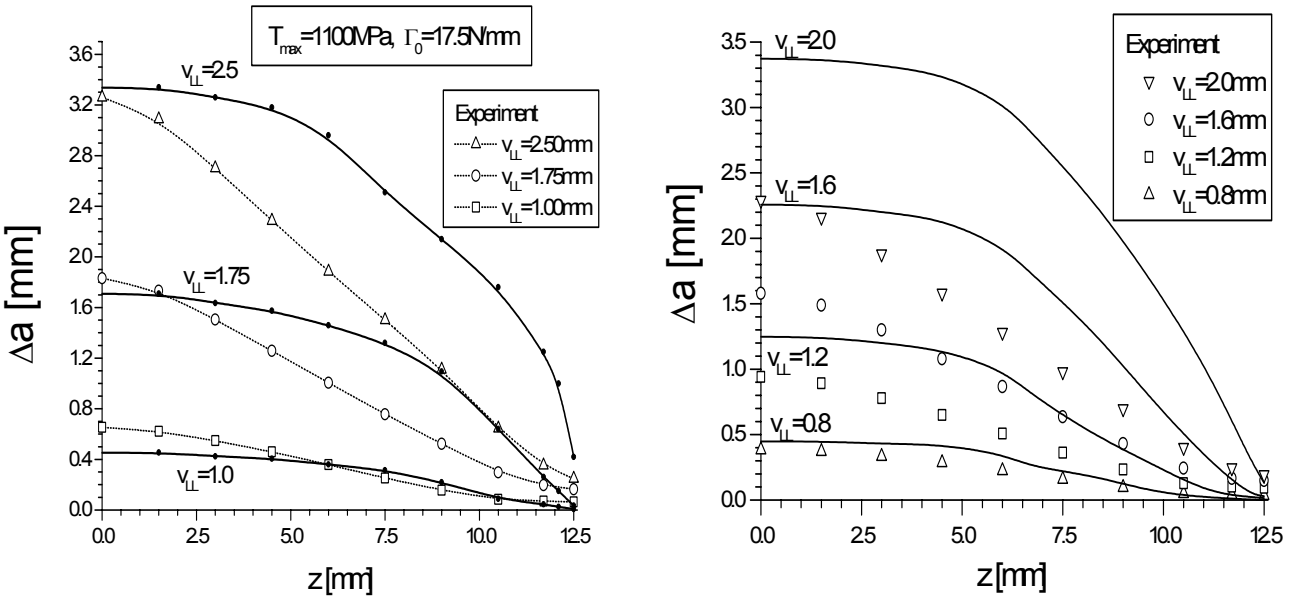

Figure 4: Comparison of the experimentally measured and the computed Δa-distribution along the crack front for three different load line displacements, v_{LL}. (a) for constant cohesive parameters, (b) for constant T_{max} and the variation of the cohesive energy, Γ_0, shown in Figure 6. *z* is the distance from the midsection.

We have seen above that only Γ_0 determines fracture initiation, i.e. $v_{LL}^{(i)}$ or J_i in the 2D case; T_{max} has no influence. As a linear relation exists between J_i and COD_i, the idea is now to measure the critical crack tip opening displacement along the crack front, $COD_i(z)$, to get a hint about the variation $\Gamma_0(z)$. COD_i is measured from corresponding regions of the fracture surface on the two specimen halves [18], applying an automatic fracture surface analysis system [19,20]. The result is shown in Figure 5. There is a midsection region of constant $COD_i^{(M)} \approx 80$ µm for $z \leq 5.5$ mm; near the side surfaces $COD_i^{(SS)} \approx 180$ µm. The ratio $COD_i^{(SS)}/COD_i^{(M)} \approx 2.2$ resembles the ratio of the separation energies $\Gamma_0^{(pl\sigma)}/\Gamma_0^{(pl\varepsilon)}$ noted above.
As a linear relation exists between the J_i and COD_i, we assume a variation of the separation energy depicted in Figure 6: For the center region of constant COD_i, $0 < z \leq 5.5$ mm, we assume $\Gamma_0(z) = \Gamma_0^{(pl\varepsilon)} = 11.5$ kJ/m^2. It seems plausible that for a valid J-resistance curve plane strain conditions prevail in the midsection region. The out-of-plane constraint decreases near the side surface. Therefore, we let the separation energy increase linearly up to a value $\Gamma_0^{(SS)} = \Gamma_0^{(pl\sigma)} = 24$ kJ/m^2 at the side surface. A constant cohesive strength of $T_{max}(z) \approx T_{max}^{(pl\varepsilon)} = 1100$ MPa is assumed for the whole specimen since the difference between $T_{max}^{(pl\varepsilon)}$ and $T_{max}^{(pl\sigma)}$ is not large and the latter value could not be determined accurately.

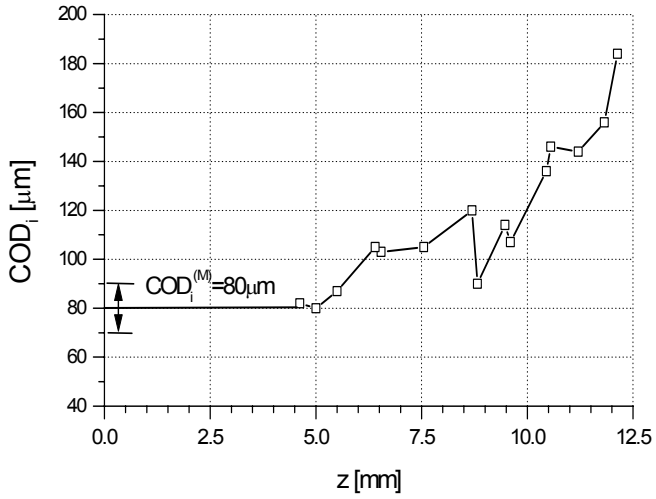

Figure 5: The variation of the critical crack tip opening displacement, COD_i, along the crack front.

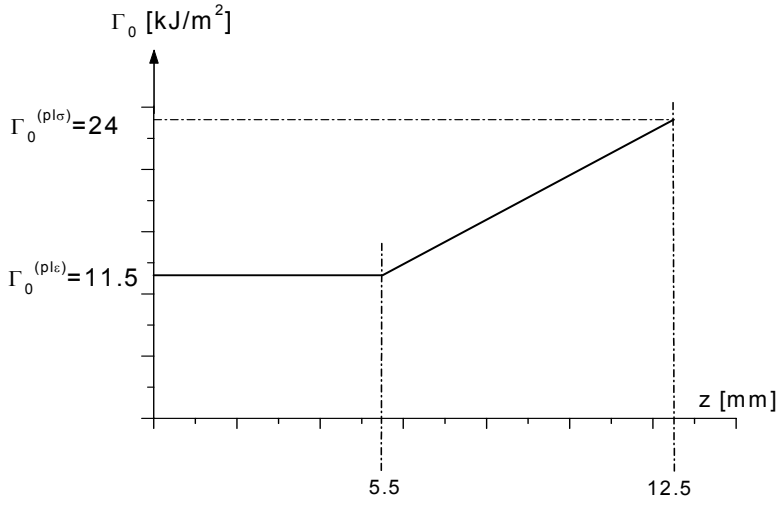

Figure 6: Assumed variation of the cohesive energy, $\Gamma_0(z)$, along the crack front for the computation shown in Figure 4b.

The result of the computation is shown in Figure 4b. The comparison between the experimental data and the computations seems to be even worse than for the case of computations with constant Γ_0. Of course, a distribution of $\Gamma_0(z)$ and $T_{max}(z)$ values could be found that would provide a better fit to the data but that is not the purpose of this paper. However, we think that important conclusions can be drawn from our two "bad" results as should be discussed in the following.

DISCUSSION

First we consider the behavior in the center region of the specimen. The value $\Gamma_0 = 11.5$ kJ/m^2 yields the correct fracture initiation behavior; also the first stages of crack extension are predicted well. With increasing v_{LL}, the crack extension becomes much too high. $\Gamma_0 = 17.5$ kJ/m^2 clearly underestimates the crack growth for small v_{LL}; however, at large v_{LL}, the crack growth rate is still overestimated. It can be concluded that it will be impossible to find any pair of constant $\Gamma_0^{(M)}$ and $T_{max}^{(M)}$ values so that the model reflects the experimental behavior. Either $\Gamma_0^{(M)}$ or $T_{max}^{(M)}$ or both must increase during the crack extension, at least, for the initial stages of crack growth. This could be due to the loss of constraint with increasing deformation [21]. The question, whether a crack growth region of constant cohesive parameters will appear after the initial transition region as it was observed in [8,9], cannot be decided yet.
Directly at the side surface, even a value of $\Gamma_0 = 17.5$ kJ/m^2 leads to a retarded crack extension for small v_{LL}. The reason might be that a too large value of the cohesive strength was taken ($T_{max} = 1100$ MPa, instead of the "correct" value for plane stress, $T_{max}^{(pl\sigma)} \approx 800$ MPa). For large v_{LL}-values, $\Gamma_0 = 17.5$ kJ/m^2 overestimates Δa, $\Gamma_0 = 24$ kJ/m^2 slightly underestimates Δa. It should be noted however, that the experimental determination of Δa is difficult and that the scatter of the data is large.
As a summary we can state that a comparison between the experimental data and the numerical simulation reveals that the parameters of the cohesive zone model depend on the location at the crack front and change during (the first stages of) crack extension.

ACKNOWLEDGEMENTS

The authors acknowledge gratefully the help of Professor W. Brocks of the GKSS Forschungszentrum Geesthacht, Germany, and the financial support of this work by the Materials Center Leoben under the project number SP7 and by the Österreichische Nationalbank under the project number 7744.

REFERENCES

1 Needleman, A. (1987) *J. Applied Mechanics* 54, 525.
2 Stüwe, H.P. (1981) In: *Three.Dimensional Constitutive Relations and Ductile Fracture,* Nemat-Nasser, S. (Ed.). North-Holland, 213.
3 Broberg, K.B. (1995) *Engng Fracture Mech.* 50, 157.
4 Ortiz, M. and Pandolfi, A. (1999) *Int. J. Numer. Mech. Engng.* 44, 1267.
5 de-Andres, A., Perez, J.L. and Ortiz, M. (1999) *Int. J. Solids Struct.* 36, 2231.
6 Tvergaard, V. and Hutchinson, J.W. (1996) *Int. J. Solids Struct.* 33, 3297.
7 Varias, A.G. (1998) *Comput. Mech.* 21, 316.
8 Siegmund, T. and Brocks, W. (1999) *Int. J. Fracture* 99, 97.
9 Siegmund, T. and Brocks, W. (2000) *ASTM STP* 1360, 139.
10 Siegmund, T. and Brocks, W. (2000) *Engng Fracture Mech.* 67, 139.
11 Kolednik, O. and Stüwe, H.P. (1986) *Engng Fracture Mech.* 24, 277.
12 Yan, W.-Y., Shan, G.X., Kolednik, O. and Fischer, F.D. (1998) *Key Engineering Materials* 145-149, 179.
13 Scheider, I. (2001) *Bruchmechanische Bewertung von Laserschweißverbindungen durch numerische Simulation mit dem Kohäsivzonenmodell.* Dissertation, Technical University Harburg, Germany.
14 ABAQUS, Version 5.7, Hibbit, Karlson & Sorenson Inc. Pawtucket, RI, USA.
15 Scheider, I. (2000) Internal Technical Paper GKSS/WMS/00/19. GKSS Forschungszentrum Geesthacht, Germany.
16 Shan, G.X., Kolednik, O., Fischer, F.D. and Stüwe, H.P. (1993) *Engng Fracture Mech.* 45, 99.
17 Kolednik, O., Shan, G.X. and Fischer, F.D. (1997) *ASTM STP* 1296, 126.
18 Kolednik, O. and Stüwe, H.P. (1985) *Engng Fracture Mech.* 21, 145.
19 Stampfl, J., Scherer, S., Berchthaler, M., Gruber, M. and Kolednik, O. (1996) *Int. J. Fracture* 78, 35.
20 Scherer, S. and Kolednik, O. (2001) *Microscopy and Analysis* 70**,** in press.
21 O'Dowd, N. and Shih, C.F. (1991) *J. Mech. Phys. Solids* 39, 898.